it is this O(carbonyl) atom at C(2) that is coordinated to the Zn atom.

References

BROOKE, J., SZABADOS, E., LYONS, S. D. & CHRISTOPHERSON, R. I. (1990). *Cancer Res.* **50**, 7793–7798.

CHRISTOPHERSON, R. I. & JONES, M. E. (1980). *J. Biol. Chem.* **255**, 3358–3370.

CHRISTOPHERSON, R. I. & LYONS, S. D. (1990). *Med. Res. Rev.* **10**, 505–548.

CHRISTOPHERSON, R. I., SCHMALZL, K. J., SZABADOS, E., GOODRIDGE, R. J., HARSANYI, M. C., SANT, M. E., ALGAR, E. M., ANDERSON, J. E., ARMSTRONG, A., SHARMA, S. C., BUBB, W. A. & LYONS, S. D. (1989). *Biochemistry*, **28**, 463–470.

FRENZ, B. A. (1985). *Enraf–Nonius Structure Determination Package*. Enraf–Nonius, Delft, The Netherlands.

HAMBLEY, T. W. (1987*a*). *J. Comput. Chem.* **8**, 651–657.

HAMBLEY, T. W. (1987*b*) *MOMEC*87. Program for strain-energy minimization. Univ. of Sydney, Australia.

HAMBLEY, T. W. (1988). *Inorg. Chem.* **27**, 1073–1077.

JOHNSON, C. K. (1965). *ORTEP*. Report ORNL-3794. Oak Ridge National Laboratory, Tennessee, USA.

KELLY, R. E., MALLY, M. I. & EVANS, D. R. (1986). *J. Biol. Chem.* **261**, 6073–6083.

SHELDRICK, G. M. (1976). *SHELX*76. Program for crystal structure determination. Univ. of Cambridge, England.

SHELDRICK, G. M. (1985). *SHELXS*86. In *Crystallographic Computing* 3, edited by G. M. SHELDRICK, C. KRÜGER & R. GODDARD, pp. 175–189. Oxford Univ. Press.

Acta Cryst. (1993). B**49**, 136–144

Structures of Riboflavin Tetraacetate and Tetrabutyrate: Molecular Packing Mode of Riboflavin Tetracarboxylate and its Extensive Stacking and Hydrogen-Bonding Characteristics

BY MATSUE EBITANI

Faculty of Engineering, Toyama University, Gofuku, Toyama 930, *Japan*

YASUKO IN AND TOSHIMASA ISHIDA*

Osaka University of Pharmaceutical Sciences, 2-10-65 *Kawai, Matsubara, Osaka* 580, *Japan*

KEN-ICHI SAKAGUCHI

Research Center for Protein Engineering, Institute for Protein Research, Osaka University, 3-2 *Yamadaoka, Suita, Osaka* 565, *Japan*

AND JUDITH L. FLIPPEN-ANDERSON* AND ISABELLA L. KARLE

Laboratory for the Structure of Matter, Naval Research Laboratory, Washington, DC 20375-5000, *USA*

(*Received* 19 *March* 1992; *accepted* 30 *June* 1992)

Abstract

Riboflavin tetraacetate (RTAc) acetone solvate monohydrate, $2C_{25}H_{28}N_4O_{10}.C_3H_6O.H_2O$, M_r = 1165.12, orthorhombic, $P2_12_12_1$, a = 61.896 (8), b = 11.424 (1), c = 8.134 (1) Å, V = 5751.5 (12) Å^3, Z = 4, D_m = 1.320 (3), D_x = 1.345 g cm^{-3}, λ(Cu $K\alpha$) = 1.5418 Å, μ = 7.84 cm^{-1}, $F(000)$ = 2456, T = 278 K, final R = 0.046 for 5060 independent observed ($F_o > 0.0$) reflections. Riboflavin tetrabutyrate (RTB), $C_{33}H_{44}N_4O_{10}$, M_r = 656.73, triclinic, $P1$, a = 19.409 (2), b = 15.332 (2), c = 11.784 (1) Å, α = 95.51 (1), β = 92.17 (1), γ = 83.59 (1)°, V = 3465.1 (6) Å^3, Z = 4, D_m = 1.250 (2), D_x = 1.259 g cm^{-3}, λ(Cu $K\alpha$) = 1.5418 Å, μ = 7.39 cm^{-1}, $F(000)$ = 1400, T = 255 K, final R = 0.094 for 6342 independent observed [$F_o > 3\sigma(F_o)$] reflections. The crystal structures of RTAc and RTB consist of two and four crystallographically independent molecules, respectively, and are stabilized by extensive stacking (aromatic spacing of 3.3–3.5 Å) and NH···O=C hydrogen-bonded dimer formation between the neighboring molecules. Each of the RTAc and RTB molecules assumes an open conformation, in order to avoid short contacts among four neighboring acetyl or butyryl groups. Although the ribityl backbones are in one of the usually observed conformations, the flexibility of the ester groups contributes to the formation of many conformers in the riboflavin derivatives. The structural characteristics inherent in the isoalloxazine ring and ribityl conformation are discussed.

* To whom all correspondence should be addressed.

0108-7681/93/010136-09$06.00

Introduction

Riboflavin not only plays a biologically important function as vitamin B_2, but also constitutes a prosthetic group of several flavoproteins that catalyse oxidation–reduction reactions as flavin mononucleotide (FMN) or flavin adenine dinucleotide (FAD), in which the isoalloxazine ring acts as the hydrogen carrier for the redox-active reaction. The isoalloxazine ring is well known to have a high propensity for forming charge-transfer complexes with biologically important aromatic compounds (Mayhew & Ludwig, 1975; McCormick, 1977; Inoue, Shibata, Kondo & Ishida, 1981; Ishida, 1988), and the π-bonding capability of the flavin ring, together with its hydrogen-bonding ability, significantly affects the physicochemical properties of crystalline riboflavin compounds. For example, the different colors of riboflavin tetracarboxylates, which are dependent on the crystallization conditions, have been discussed in connection with ring stacking or hydrogen-bonding modes (Ebitani, Kashiwagi, Inoue, Enomoto & Ishida, 1989). As a continuation of studies elucidating the relationship between the interaction mode of neighboring flavins and crystal color at atomic level, this paper deals with the crystal structures of riboflavin tetraacetate (RTAc) and tetrabutyrate (RTB); the comparative study of RTAc and RTB crystal structures also affords information as to the relationship between the bulkiness of ester groups and the molecular packing mode. The atomic numbering used is shown in Fig. 1.

Riboflavin tetracarboxylates such as RTB and RTAc are used as drugs for hyperlipemia and as food additives (Ishidate, 1979). Crystals of three different colors are formed depending upon the crystallization conditions, *i.e.* orange (*A*-type), dark-yellow (*B*-type) and yellow (*C*-type) crystals (Ebitani, 1987, 1988*a*,*b*). Since molecules in these crystals aggregate in a similar fashion, as judged from the NMR, mass and powder X-ray diffraction spectra, the color changes are primarily dependent on the differences among the molecular packing modes.

Experimental

Preparation of RTAc and RTB crystals

RTAc and RTB were synthesized by the esterification of riboflavin by acetic acid and *n*-butyric acid, respectively, according to Ebitani (1987, 1988*b*). Orange platelet crystals of *A*-type RTB and RTAc were crystallized from ethanol and 50% aqueous acetone solutions, respectively, by slow evaporation at room temperature (293 K). Since the crystals became opaque on standing in air, they were sealed in glass capillaries containing some mother liquor. The crystal density was measured by the flotation method in a CCl_4/C_6H_6 mixture. There are two and four crytallographically independent molecules per asymmetric unit for RTAc and RTB crystals, respectively, and they were named as molecules *A* and *B* for RTAc molecules and molecules *A*, *B*, *C* and *D* for RTB molecules.

Data collection and structure analysis of RTAc

Cell dimensions were determined by a least-squares fit of 25 reflections ($2\theta = 30$–$55°$). A total of 5608 independent intensity data in the 2θ range 2–130° ($\sin\theta/\lambda < 0.588$ Å^{-1}) were measured using a platelet crystal (dimensions $0.3 \times 0.4 \times 0.1$ mm) and a Rigaku AFC-5 diffractometer with graphite-monochromated Cu $K\alpha$ radiation; range of hkl: $0 \le h \le 73$, $0 \le k \le 13$, $-9 \le l \le 0$. The θ–2θ mode was used with a scan width of $(1.40 + 0.15\tan\theta)°$ and a scan speed of 3° min^{-1} in θ; the background was counted for 5 s at both edges of a reflection. Since four standard reflections (32,0,0, 060, 004 and 344) monitored at 100 reflection intervals decreased as a function of measuring time, the intensities were corrected based on the decreasing curve. Lorentz and polarization corrections were also applied. The structure solution and refinement were carried out using 5060 independent reflections with $F_o > 0.0$.

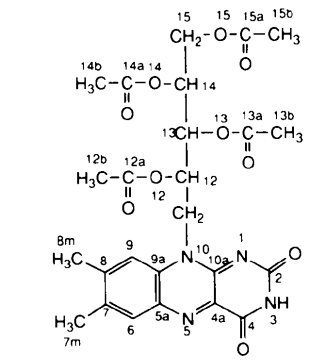

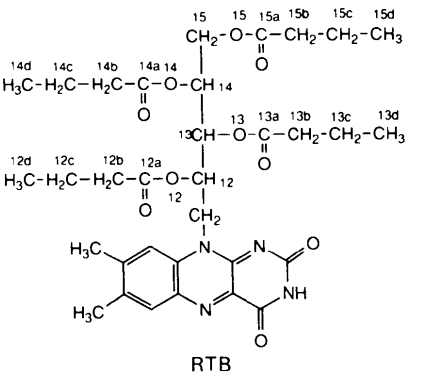

Fig. 1. Chemical structures and atomic numbering schemes of RTAc and RTB molecules.

The structure was solved by a combination of a Patterson rigid-body vector search of two antiparallel stacked isoalloxazine rings and the direct-methods program *MULTAN*87 (Debaerdemaeker, Germain, Main, Tate & Woolfson, 1987). Solvent water and acetone molecules were located by successive Fourier syntheses. Atomic coordinates for H atoms were calculated on the basis of stereochemical considerations and most of them, except the methyl or methylene groups showing relatively high thermal motions, were also located on a difference Fourier map. The structure was refined by the block-diagonal least-squares method with anisotropic temperature factors for non-H atoms and isotropic factors for H atoms (except for those of solvents), where the function $\sum w(|F_o| - |F_c|)^2$ was minimized. 973 parameters were refined. In the final refinement, $w = 1.0/[\sigma^2(|F_o|) - 0.10159|F_o| + 0.0012|F_o|^2]$ was used. Final $R = 0.046$ and $wR = 0.086$, $(\Delta/\sigma)_{max} = 0.88$, ratio of observations to parameters = 5.2. $(\Delta\rho) = -0.25$–0.31 e Å^{-3}, S (goodness of fit) = 0.916. Final coordinates and B_{eq} values for the non-H atoms are given in Table 1. *The Universal Crystallographic Computing System – Osaka* (1979) was used for all crystallographic computations.

Data collection and structure analysis of RTB

A translucent orange prism (0.12 × 0.20 × 0.25 mm) recrystallized from ethanol was used for data collection on an automated Siemens *R*3*m*/*V* diffractometer with an incident beam monochromator (Cu $K\alpha$ radiation). 25 centered reflections within $21 < 2\theta < 26°$ were used for determining lattice parameters. $(\sin\theta/\lambda)_{max} = 0.54$ Å^{-1}, range of *hkl*: $-20 \le h \le 0$, $-16 \le k \le 16$, $-12 \le l \le 11$. Standards 300, 050, 003, monitored every 97 reflections with random variation of 2.5% over data collection, θ–2θ scan mode, scan width $[2\theta(K\alpha_1) - 1.0]$ to $[2\theta(K\alpha_2) + 1.0]°$, constant scan rate (10.0° min^{-1}), 10711 reflections measured, 8312 unique, $R_{int} = 0.96\%$, 6342 observed with $F_o > 3\sigma(F_o)$. Data were corrected for Lorentz and polarization effects.

The structure was solved by direct methods. Many of the E maps calculated from random phase-set assignments showed planar groups of several fused six-membered rings making it difficult to find a suitable structural fragment for tangent-formula expansion. Finally, 30 atoms were selected from an E map which showed a chain of atoms out of the plane of one of the six-membered ring fragments. Even though several of these atoms were later shown to be spurious, it was possible with many iterations of alternating tangent-formula expansion and adjustment of the model to determine the entire 188-atom structure. Both the structure solution and the full-matrix least-squares refinement used programs in *SHELXTL* (Sheldrick, 1980). $\sum w(|F_o| - |F_c|)^2$ was minimized, where $w = 1/[\sigma^2(|F_o|) + 0.001(F_o)^2]$. 1533 parameters were refined: atomic coordinates for all non-H atoms, isotropic thermal parameters for the two C atoms at the end of each chain, anisotropic thermal parameters for the remaining non-H atoms, and H atoms with the fixed isotropic parameter included using the riding model (coordinate shifts of C applied to attached H atoms, C—H distance set to 0.96 Å, H angles idealized). Because of the high thermal parameters for many of the atoms towards the ends of the butyryl ester chains, it was necessary to restrain the C—C bond lengths during the refinement [C—C bond lengths restrained to 1.520 (2) Å and C···C skip distances restrained to 2.500 (8) Å]. This is also a cause of the relatively high values of $R = 0.094$ and $wR = 0.105$. $(\Delta/\sigma)_{max} = 0.95$, ratio of observations to parameters = 4.1, $S = 2.00$. Final difference Fourier excursions 0.67 and −0.39 e Å^{-3}. The final atomic coordinates and U_{eq} values for the non-H atoms are given in Table 2.*

Atomic scattering factors taken from *International Tables for X-ray Crystallography* (1974, Vol. IV) were used for the calculations for RTAc and RTB structure factors. The relationship between B and U values for the thermal parameters is $B = 8\pi^2 U$.

Results and discussion

Figs. 2 and 3 show stereoscopic views of the RTAc and RTB molecular conformations, respectively. Stereoscopic molecular packing diagrams of RTAc and RTB crystals are shown in Fig. 4. Extensive overlapping and hydrogen-bonding modes among the neighboring isoalloxazine rings are shown in Figs. 5 and 6. Selected torsion angles involving the ribityl group are given in Table 3. Possible hydrogen bonds are summarized in Table 4.

Conformational features and crystal packing of the RTAc molecule

The bond lengths and angles have standard deviations of 0.005–0.01 Å and 0.2–0.4°, respectively, and agree well with those of related flavins. The isoalloxazine ring forms a plane with an r.m.s. deviation of 0.01 Å for molecule *A* and 0.02 Å for molecule *B*, and the planarities of both rings are reasonable. The

* Lists of structure factors, anisotropic temperature factors, H-atom parameters, bond lengths and angles, torsion angles, short contacts between the stacking isoalloxazine rings less than 3.45 Å, and the planarities of isoalloxazine rings and dihedral angles between the rings for the RTAc and RTB crystals have been deposited with the British Library Document Supply Centre as Supplementary Publication No. SUP 55506 (74 pp.). Copies may be obtained through The Technical Editor, International Union of Crystallography, 5 Abbey Square, Chester CH1 2HU, England.

Table 1. *Fractional coordinates with e.s.d.'s and equivalent isotropic temperature factors of RTAc*

$B_{eq} = (4/3)\Sigma_i\Sigma_j \beta_{ij} \mathbf{a}_i.\mathbf{a}_j$.

	x	y	z	B_{eq} (Å^2)
Molecule *A*				
N(1)	0.89573 (4)	−0.1443 (3)	0.5145 (4)	3.2 (1)
C(2)	0.88541 (6)	−0.2524 (3)	0.5063 (5)	3.4 (2)
O(2)	0.89360 (4)	−0.3356 (2)	0.4381 (4)	4.4 (1)
N(3)	0.86534 (5)	−0.2656 (3)	0.5795 (5)	3.7 (1)
C(4)	0.85361 (5)	−0.1822 (3)	0.6577 (6)	3.6 (2)
O(4)	0.83582 (4)	0.1980 (3)	0.7108 (5)	5.9 (2)
C(4a)	0.86540 (5)	−0.0672 (3)	0.6719 (5)	3.2 (1)
N(5)	0.85595 (4)	0.0166 (3)	0.7511 (4)	3.2 (1)
C(5a)	0.86677 (5)	0.1214 (3)	0.7592 (5)	3.2 (1)
C(6)	0.85653 (6)	0.2145 (4)	0.8393 (6)	3.9 (2)
C(7)	0.86629 (6)	0.3253 (4)	0.8554 (5)	3.8 (2)
C(7*m*)	0.85411 (6)	0.4248 (4)	0.9400 (6)	4.8 (2)
C(8)	0.88740 (6)	0.3385 (4)	0.7872 (6)	3.8 (2)
C(8*m*)	0.89836 (7)	0.4544 (4)	0.8026 (7)	5.1 (2)
C(9)	0.89761 (5)	0.2472 (3)	0.7073 (5)	3.3 (2)
C(9a)	0.88727 (5)	0.1382 (3)	0.6913 (5)	3.0 (1)
N(10)	0.89652 (4)	0.0457 (3)	0.6024 (4)	3.0 (1)
C(10a)	0.88627 (5)	−0.0596 (3)	0.5961 (5)	2.9 (1)
C(11)	0.91677 (5)	0.0621 (3)	0.5137 (5)	3.0 (1)
C(12)	0.93741 (5)	0.0432 (3)	0.6152 (5)	2.9 (1)
O(12)	0.94248 (3)	−0.0808 (2)	0.6145 (3)	3.3 (1)
C(12a)	0.93368 (5)	−0.1453 (3)	0.7364 (6)	3.5 (2)
O(12a)	0.92331 (4)	−0.1052 (3)	0.8429 (4)	4.5 (1)
C(12b)	0.93843 (7)	−0.2735 (4)	0.7097 (8)	5.3 (2)
C(13)	0.95641 (5)	0.1029 (3)	0.5301 (5)	2.8 (1)
O(13)	0.95206 (3)	0.2267 (2)	0.5609 (3)	3.2 (1)
C(13a)	0.96032 (6)	0.3042 (4)	0.4488 (6)	4.2 (2)
O(13a)	0.97172 (6)	0.2735 (3)	0.3381 (4)	5.8 (2)
C(13b)	0.95435 (8)	0.4295 (4)	0.4908 (8)	6.0 (2)
C(14)	0.97910 (4)	0.0734 (4)	0.5921 (5)	3.1 (1)
O(14)	0.97857 (3)	0.0806 (2)	0.7715 (3)	3.5 (1)
C(14a)	0.99446 (6)	0.1433 (4)	0.8474 (5)	3.7 (2)
O(14a)	1.00908 (4)	0.1835 (4)	0.7709 (5)	6.2 (2)
C(14b)	0.99095 (7)	0.1481 (4)	1.0266 (6)	4.7 (2)
C(15)	0.98685 (5)	−0.0468 (4)	0.5415 (7)	4.3 (2)
O(15)	1.00991 (3)	−0.0600 (3)	0.5749 (4)	4.1 (1)
C(15a)	1.02340 (6)	−0.0187 (4)	0.4613 (6)	3.9 (2)
O(15a)	1.01770 (5)	0.0343 (3)	0.3432 (5)	5.5 (2)
C(15b)	1.04630 (6)	−0.0470 (5)	0.5057 (7)	5.3 (2)
Molecule *B*				
N(1)	0.84670 (4)	0.3186 (3)	0.4367 (5)	3.7 (1)
C(2)	0.85791 (5)	0.4218 (4)	0.4489 (5)	3.6 (2)
O(2)	0.85071 (5)	0.5053 (2)	0.5244 (5)	5.1 (1)
N(3)	0.87790 (4)	0.4328 (3)	0.3756 (5)	3.8 (1)
C(4)	0.88831 (6)	0.3458 (3)	0.2948 (5)	3.7 (2)
O(4)	0.90671 (4)	0.3585 (3)	0.2353 (5)	5.4 (2)
C(4a)	0.87642 (6)	0.2340 (4)	0.2835 (5)	3.4 (2)
N(5)	0.88536 (4)	0.1460 (3)	0.2078 (4)	3.3 (1)
C(5a)	0.87408 (5)	0.0425 (3)	0.2015 (5)	2.9 (1)
C(6)	0.88296 (6)	−0.0511 (4)	0.1186 (5)	3.8 (2)
C(7)	0.87260 (5)	−0.1574 (3)	0.1105 (5)	3.3 (2)
C(7*m*)	0.88319 (7)	−0.2602 (4)	0.0207 (7)	4.7 (2)
C(8)	0.85250 (5)	−0.1730 (3)	0.1893 (5)	3.4 (2)
C(8*m*)	0.84047 (6)	−0.2864 (4)	0.1799 (7)	4.5 (2)
C(9)	0.84354 (5)	−0.0799 (4)	0.2699 (5)	3.4 (2)
C(9a)	0.85369 (5)	0.0286 (3)	0.2793 (5)	3.0 (1)
N(10)	0.84511 (4)	0.1250 (3)	0.3621 (4)	3.2 (1)
C(10a)	0.85580 (5)	0.2309 (3)	0.3627 (5)	3.1 (1)
C(11)	0.82466 (5)	0.1166 (3)	0.4569 (5)	3.3 (2)
C(12)	0.80527 (5)	0.1503 (4)	0.3559 (5)	3.5 (2)
O(12)	0.80263 (4)	0.0656 (3)	0.2283 (4)	4.0 (1)
C(12a)	0.80251 (9)	0.0952 (5)	0.0701 (7)	5.8 (3)
O(12a)	0.8063 (1)	0.1892 (6)	0.0320 (7)	13.3 (4)
C(12b)	0.80081 (9)	0.0034 (6)	−0.0425 (8)	6.9 (3)
C(13)	0.78483 (5)	0.1555 (4)	0.4579 (6)	3.6 (2)
O(13)	0.78303 (4)	0.0418 (2)	0.5351 (4)	3.8 (1)
C(13a)	0.76711 (6)	0.0295 (4)	0.4903 (7)	4.8 (2)
O(13a)	0.75320 (6)	−0.0022 (4)	0.3900 (6)	7.6 (2)
C(13b)	0.76832 (9)	−0.1430 (5)	0.5723 (8)	6.3 (3)
C(14)	0.78446 (6)	0.2445 (4)	0.5946 (6)	4.0 (2)
O(14)	0.78917 (5)	0.3545 (3)	0.5122 (5)	4.9 (1)
C(14a)	0.79841 (7)	0.4374 (5)	0.6066 (8)	5.4 (2)
O(14a)	0.80378 (7)	0.4243 (4)	0.7440 (5)	7.5 (2)
C(14b)	0.80020 (9)	0.5510 (4)	0.5149 (9)	6.6 (3)
C(15)	0.76357 (7)	0.2535 (5)	0.6851 (8)	5.5 (2)
O(15)	0.74720 (5)	0.2897 (4)	0.5534 (6)	7.3 (2)
C(15a)	0.7277 (1)	0.309 (1)	0.578 (1)	11.8 (6)
O(15a)	0.71986 (9)	0.2620 (7)	0.7059 (9)	12.9 (4)
C(15b)	0.7144 (1)	0.3525 (9)	0.449 (1)	11.7 (6)
Solvent				
C(1Ac)	0.97248 (8)	0.8330 (6)	1.0653 (7)	6.3 (3)
C(2Ac)	0.95249 (7)	0.8571 (4)	1.1659 (6)	4.4 (2)
C(3Ac)	0.9406 (1)	0.7563 (6)	1.2315 (9)	7.0 (3)
O(1Ac)	0.94612 (6)	0.9554 (3)	1.187 (5)	6.4 (2)
O(1*W*)	0.93110 (6)	1.1706 (4)	1.0123 (6)	7.3 (2)

dihedral angle between the benzene and uracil moieties is 1.6 (2)° for molecule *A* and 2.4 (2)° for molecule *B*. Some acetyl esters in molecule *B* show large thermal motions because of no direct participation in any specific interaction such as hydrogen-bond formation, and of the relatively loose short contacts. The conformational characteristics of the ribityl side chain can be described by the torsion angles χ_1 to χ_5 (Table 3). There are two independent rotational isomers around the N(10)—C(11) bond. The torsion angles of $\chi_1 \simeq 90°$ (*P* conformation) or $\simeq -90°$ (*M* conformation) have been found to be favored in the riboflavin conformation when the χ_2 torsion angle is in a *trans* region (Fujii, Kawasaki, Sato, Fujiwara & Tomita, 1977). The conformation of RTAc also follows this rule, that is, the *M* conformation for molecule *A* and the *P* conformation for molecule *B*. Nearly the same populations of *P* and *M* conformers have been found so far in the crystal structures of riboflavin analogues, including isolated and complexed crystals. This indicates the same preference for both conformations and could account for the reason why many crystals of riboflavin analogues contain more than two crystallographically independent molecules per asymmetric unit. The torsion angle χ_2 is almost limited to the *trans* region, as a result of the *P* or *M* conformation of χ_1. No specific preference is observed concerning the torsion angles χ_3 to χ_5. They are found to be in the *gauche*$^+$, *gauche*$^-$ or *trans* regions. The *gauche*$^+$ or *gauche*$^-$ conformation, with the aid of the *trans* conformation of adjacent bonds at each side, avoids intramolecular short contacts, especially between the acetyl ester moieties, and leads to the nonplanar and non-*trans* zigzag conformations of the carbon atoms in the ribityl backbone (Fig. 2). This is in contrast with the FMN or FAD conformation bound in the active site of an enzyme (for example, Schulz, Schirmer & Pai, 1982; Karplus & Schulz, 1987; Schrender, Prick, Wierenga, Vriend, Wilson, Hol & Drenth, 1989; Vrielink, Lloyd & Blow, 1991), where an extended *trans* conformation has been commonly observed.

Fig. 4(*a*) shows the characteristic packing mode of RTAc molecules. The crystal consists of alternate layers of isoalloxazine and ribityl moieties, which run

Table 2. *Fractional coordinates with e.s.d.'s and equivalent isotropic temperature factors of RTB*

$$U_{eq} = (1/3)\sum_i \sum_j U_{ij} a_i^* a_j^* \mathbf{a}_i . \mathbf{a}_j .$$

	x	y	z	U_{eq} (Å^2)
Molecule *A*				
N(1)	0.9309 (5)	1.0384 (7)	0.6230 (9)	0.061 (7)
C(2)	0.9577 (7)	0.993 (1)	0.526 (1)	0.07 (1)
O(2)	0.9630 (6)	1.0314 (7)	0.4392 (8)	0.092 (7)
N(3)	0.9781 (5)	0.9041 (8)	0.5248 (9)	0.070 (8)
C(4)	0.9794 (7)	0.853 (1)	0.613 (1)	0.06 (1)
O(4)	1.0051 (5)	0.7772 (6)	0.6062 (7)	0.077 (6)
C(4a)	0.9464 (6)	0.9008 (8)	0.717 (1)	0.046 (8)
N(5)	0.9409 (5)	0.8581 (6)	0.804 (1)	0.055 (7)
C(5a)	0.9139 (6)	0.9054 (8)	0.904 (1)	0.050 (8)
C(6)	0.9059 (7)	0.8575 (9)	0.996 (1)	0.061 (9)
C(7)	0.8809 (7)	0.901 (1)	1.094 (1)	0.07 (1)
C(7*m*)	0.8744 (8)	0.848 (1)	1.195 (1)	0.10 (1)
C(8)	0.8642 (7)	0.992 (1)	1.106 (1)	0.07 (1)
C(8*m*)	0.8394 (8)	1.043 (1)	1.213 (1)	0.09 (1)
C(9)	0.8734 (6)	1.0384 (9)	1.011 (1)	0.058 (9)
C(9a)	0.8972 (6)	0.9955 (7)	0.906 (1)	0.049 (8)
N(10)	0.9041 (5)	1.0398 (6)	0.8123 (8)	0.051 (7)
C(10a)	0.9284 (6)	0.9954 (8)	0.712 (1)	0.049 (8)
C(11)	0.8856 (6)	1.1377 (7)	0.8190 (9)	0.050 (8)
C(12)	0.8105 (6)	1.1641 (7)	0.804 (1)	0.051 (8)
O(12)	0.7840 (4)	1.1365 (6)	0.6920 (8)	0.067 (6)
C(12a)	0.7625 (8)	1.058 (1)	0.666 (1)	0.09 (1)
O(12a)	0.7583 (6)	1.0099 (6)	0.739 (1)	0.093 (8)
C(12b)	0.7425 (9)	1.044 (1)	0.540 (1)	0.17 (2)
C(12c)	0.674 (1)	1.097 (2)	0.516 (2)	0.23 (1)†
C(12d)	0.652 (2)	1.081 (3)	0.391 (2)	0.35 (2)†
C(13)	0.7932 (7)	1.2664 (8)	0.825 (1)	0.059 (9)
O(13)	0.7328 (4)	1.2894 (5)	0.8896 (7)	0.058 (6)
C(13a)	0.7397 (8)	1.2825 (9)	1.004 (1)	0.09 (1)
O(13a)	0.7975 (7)	1.2540 (7)	1.0439 (8)	0.101 (8)
C(13b)	0.6736 (7)	1.3179 (9)	1.066 (1)	0.09 (1)
C(13c)	0.682 (1)	1.307 (1)	1.1928 (9)	0.157 (8)†
C(13d)	0.653 (2)	1.223 (2)	1.219 (2)	0.34 (2)†
C(14)	0.7811 (7)	1.3112 (8)	0.719 (1)	0.068 (9)
O(14)	0.8431 (5)	1.2909 (6)	0.657 (1)	0.086 (7)
C(14a)	0.838 (1)	1.282 (1)	0.544 (2)	0.12 (2)
O(14a)	0.7804 (8)	1.2925 (9)	0.491 (1)	0.15 (1)
C(14b)	0.9074 (8)	1.252 (1)	0.491 (1)	0.14 (2)
C(14c)	0.907 (1)	1.275 (1)	0.368 (1)	0.21 (1)†
C(14d)	0.918 (2)	1.371 (2)	0.366 (3)	0.36 (2)†
C(15)	0.7642 (7)	1.4111 (8)	0.735 (1)	0.08 (1)
O(15)	0.8235 (5)	1.4465 (6)	0.7905 (9)	0.095 (8)
C(15a)	0.8270 (8)	1.535 (1)	0.787 (2)	0.10 (1)
O(15a)	0.7776 (6)	1.5784 (6)	0.742 (1)	0.128 (9)
C(15b)	0.8919 (8)	1.567 (1)	0.845 (1)	0.14 (2)
C(15c)	0.9318 (9)	1.612 (1)	0.762 (2)	0.159 (8)†
C(15d)	0.953 (1)	1.548 (2)	0.659 (2)	0.22 (1)†
Molecule *B*				
N(1)	0.5336 (7)	0.6079 (9)	1.110 (1)	0.09 (1)
C(2)	0.508 (1)	0.574 (1)	1.200 (2)	0.11 (2)
O(2)	0.4985 (7)	0.6169 (8)	1.294 (1)	0.12 (1)
N(3)	0.4917 (6)	0.4877 (9)	1.195 (1)	0.10 (1)
C(4)	0.4953 (8)	0.427 (1)	1.098 (2)	0.10 (1)
O(4)	0.4794 (6)	0.3548 (8)	1.093 (1)	0.122 (9)
C(4a)	0.5241 (7)	0.465 (1)	1.000 (2)	0.08 (1)
N(5)	0.5326 (6)	0.4134 (8)	0.907 (1)	0.083 (9)
C(5a)	0.5589 (7)	0.448 (1)	0.817 (2)	0.08 (1)
C(6)	0.5684 (8)	0.390 (1)	0.713 (2)	0.09 (1)
C(7)	0.5891 (7)	0.423 (1)	0.615 (2)	0.09 (1)
C(7*m*)	0.5987 (9)	0.364 (1)	0.505 (2)	0.13 (2)
C(8)	0.6055 (8)	0.512 (1)	0.623 (2)	0.10 (1)
C(8*m*)	0.6310 (8)	0.551 (1)	0.522 (1)	0.11 (1)
C(9)	0.5954 (7)	0.570 (1)	0.726 (2)	0.09 (1)
C(9a)	0.5740 (7)	0.536 (1)	0.825 (2)	0.08 (1)
N(10)	0.5646 (6)	0.5886 (7)	0.925 (1)	0.077 (9)
C(10a)	0.5400 (7)	0.554 (1)	1.017 (2)	0.08 (1)
C(11)	0.5794 (7)	0.6831 (9)	0.9032 (1)	0.09 (1)
C(12)	0.6546 (8)	0.6905 (9)	0.936 (2)	0.10 (1)
O(12)	0.6835 (6)	0.6727 (6)	1.048 (1)	0.117 (9)
C(12a)	0.710 (1)	0.588 (1)	1.064 (2)	0.13 (2)
O(12a)	0.7096 (6)	0.5302 (7)	0.988 (1)	0.111 (9)
C(12b)	0.729 (2)	0.587 (2)	1.191 (2)	0.25 (3)
C(12c)	0.806 (1)	0.565 (4)	1.208 (3)	0.49 (4)†
C(12d)	0.821 (3)	0.482 (6)	1.27 (1)	1.31 (8)†
C(13)	0.6670 (8)	0.7904 (9)	0.926 (2)	0.10 (1)
O(13)	0.7268 (5)	0.7890 (6)	0.855 (1)	0.094 (8)
C(13a)	0.7142 (7)	0.7747 (9)	0.738 (1)	0.10 (1)
O(13a)	0.6598 (6)	0.7544 (7)	0.697 (1)	0.114 (9)
C(13b)	0.7771 (6)	0.7870 (9)	0.670 (1)	0.10 (1)
C(13c)	0.7701 (8)	0.748 (1)	0.548 (1)	0.121 (6)†
C(13d)	0.8304 (8)	0.766 (1)	0.479 (1)	0.139 (7)†
C(14)	0.6844 (9)	0.8422 (9)	1.040 (2)	0.10 (1)
O(14)	0.6230 (5)	0.8438 (6)	1.109 (1)	0.112 (9)
C(14a)	0.635 (1)	0.834 (1)	1.227 (2)	0.11 (2)
O(14a)	0.6901 (7)	0.837 (1)	1.259 (1)	0.14 (1)
C(14b)	0.5664 (7)	0.824 (1)	1.280 (1)	0.12 (2)
C(14c)	0.577 (1)	0.805 (1)	1.404 (1)	0.151 (8)†
C(14d)	0.582 (2)	0.890 (2)	1.481 (2)	0.31 (2)†
C(15)	0.6975 (8)	0.937 (1)	1.018 (2)	0.12 (1)
O(15)	0.6405 (6)	0.9738 (8)	0.953 (2)	0.17 (1)
C(15a)	0.656 (2)	1.061 (3)	0.938 (4)	0.25 (5)
O(15a)	0.685 (2)	1.098 (1)	0.984 (3)	0.23 (2)
C(15b)	0.584 (2)	1.109 (2)	0.919 (3)	0.48 (3)
C(15c)	0.552 (2)	1.074 (3)	0.805 (3)	0.37 (3)†
C(15d)	0.486 (2)	1.131 (3)	0.778 (3)	0.45 (3)†
Molecule *C*				
N(1)	0.4070 (6)	0.4419 (7)	0.579 (1)	0.074 (8)
C(2)	0.4271 (7)	0.4823 (9)	0.490 (2)	0.07 (1)
O(2)	0.4347 (6)	0.4436 (6)	0.398 (1)	0.105 (9)
N(3)	0.4432 (6)	0.5680 (8)	0.506 (1)	0.079 (8)
C(4)	0.4382 (6)	0.623 (1)	0.608 (2)	0.07 (1)
O(4)	0.4547 (5)	0.6976 (7)	0.616 (1)	0.109 (8)
C(4a)	0.4127 (7)	0.580 (1)	0.704 (2)	0.07 (1)
N(5)	0.4072 (6)	0.6237 (7)	0.797 (1)	0.079 (9)
C(5a)	0.3815 (7)	0.5876 (9)	0.885 (1)	0.07 (1)
C(6)	0.3671 (8)	0.633 (1)	0.993 (2)	0.09 (1)
C(7)	0.3375 (9)	0.600 (1)	1.081 (2)	0.10 (1)
C(7*m*)	0.3246 (9)	0.658 (1)	1.189 (1)	0.12 (1)
C(8)	0.3246 (9)	0.514 (2)	1.067 (2)	0.10 (1)
C(8*m*)	0.292 (1)	0.469 (1)	1.158 (1)	0.11 (1)
C(9)	0.3390 (8)	0.462 (1)	0.969 (2)	0.09 (1)
C(9a)	0.3678 (7)	0.4950 (8)	0.876 (1)	0.064 (9)
N(10)	0.3829 (5)	0.4474 (7)	0.771 (1)	0.064 (7)
C(10a)	0.3995 (7)	0.4875 (9)	0.683 (2)	0.07 (1)
C(11)	0.3812 (6)	0.3512 (7)	0.761 (1)	0.064 (8)
C(12)	0.3106 (7)	0.3199 (8)	0.727 (1)	0.069 (9)
O(12)	0.3057 (5)	0.2396 (5)	0.7802 (8)	0.071 (6)
C(12a)	0.2659 (7)	0.2434 (8)	0.873 (1)	0.09 (1)
O(12a)	0.2382 (7)	0.3074 (8)	0.919 (1)	0.13 (1)
C(12b)	0.2653 (9)	0.1510 (7)	0.909 (1)	0.11 (1)
C(12c)	0.2326 (9)	0.1544 (9)	1.025 (1)	0.124 (6)†
C(12d)	0.245 (1)	0.065 (1)	1.073 (2)	0.19 (1)†
C(13)	0.3019 (7)	0.3014 (8)	0.605 (1)	0.064 (9)
O(13)	0.2302 (5)	0.2926 (6)	0.5711 (8)	0.077 (6)
C(13a)	0.192 (1)	0.360 (1)	0.543 (2)	0.20 (2)
O(13a)	0.2020 (9)	0.434 (1)	0.590 (2)	0.20 (2)
C(13b)	0.1202 (7)	0.347 (1)	0.490 (2)	0.13 (2)
C(13c)	0.126 (1)	0.302 (2)	0.370 (2)	0.24 (1)†
C(13d)	0.172 (2)	0.349 (2)	0.300 (2)	0.30 (2)†
C(14)	0.3425 (7)	0.2180 (9)	0.553 (1)	0.08 (1)
O(14)	0.3643 (6)	0.2283 (6)	0.4412 (9)	0.091 (8)
C(14a)	0.432 (1)	0.227 (1)	0.428 (1)	0.10 (2)
O(14a)	0.4756 (6)	0.2163 (8)	0.499 (1)	0.115 (9)
C(14b)	0.453 (1)	0.236 (1)	0.307 (2)	0.13 (2)
C(14c)	0.424 (1)	0.167 (2)	0.223 (2)	0.25 (2)†
C(14d)	0.472 (2)	0.082 (1)	0.214 (3)	0.32 (2)†
C(15)	0.3045 (8)	0.1350 (8)	0.549 (2)	0.10 (1)
O(15)	0.3530 (6)	0.0596 (7)	0.516 (1)	0.118 (9)
C(15a)	0.344 (1)	−0.014 (1)	0.552 (2)	0.12 (2)
O(15a)	0.2990 (8)	−0.0157 (8)	0.618 (1)	0.15 (1)
C(15b)	0.390 (1)	−0.095 (1)	0.504 (2)	0.27 (3)
C(15c)	0.390 (1)	0.101 (2)	0.374 (2)	0.45 (3)†
C(15d)	0.318 (2)	0.105 (3)	0.323 (2)	0.36 (2)†
Molecule *D*				
N(1)	1.0735 (5)	0.8596 (7)	1.1141 (9)	0.062 (7)
C(2)	1.0523 (8)	0.897 (1)	1.221 (1)	0.08 (1)
O(2)	1.0449 (5)	0.8478 (7)	1.2965 (7)	0.088 (7)
N(3)	1.0362 (6)	0.9848 (9)	1.245 (1)	0.077 (9)
C(4)	1.0403 (8)	1.047 (1)	1.169 (1)	0.08 (1)
O(4)	1.0232 (7)	1.1261 (7)	1.1964 (9)	0.119 (9)
C(4a)	1.0621 (6)	1.0125 (8)	1.056 (1)	0.047 (8)
N(5)	1.0642 (6)	1.0657 (6)	0.979 (1)	0.070 (7)
C(5a)	1.0841 (6)	1.0299 (8)	0.873 (1)	0.062 (9)
C(6)	1.0890 (7)	1.0887 (9)	0.790 (1)	0.07 (1)
C(7)	1.1082 (7)	1.057 (1)	0.681 (1)	0.07 (1)
C(7*m*)	1.1082 (8)	1.127 (1)	0.588 (1)	0.11 (1)
C(8)	1.1235 (6)	0.9665 (9)	0.651 (1)	0.065 (9)
C(8*m*)	1.1449 (8)	0.930 (1)	0.534 (1)	0.10 (1)
C(9)	1.1201 (6)	0.9089 (8)	0.735 (1)	0.060 (8)
C(9a)	1.0996 (6)	0.9397 (8)	0.845 (1)	0.047 (8)
N(10)	1.0925 (4)	0.8841 (5)	0.9306 (8)	0.045 (6)

Table 2 (*cont.*)

	x	*y*	*z*	U_{eq} (Å^2)		*x*	*y*	*z*	U_{eq} (Å^2)
C(10a)	1.0770 (6)	0.9183 (8)	1.041 (1)	0.051 (8)	C(13d)	1.2757 (9)	0.706 (1)	0.500 (2)	0.152 (8)†
C(11)	1.0950 (6)	0.7848 (7)	0.897 (1)	0.049 (7)	C(14)	1.1184 (7)	0.5904 (8)	0.923 (1)	0.07 (1)
C(12)	1.1675 (5)	0.7390 (7)	0.924 (1)	0.051 (7)	O(14)	1.1247 (5)	0.6031 (5)	1.0481 (8)	0.074 (6)
O(12)	1.2191 (4)	0.7753 (5)	0.8628 (7)	0.056 (5)	C(14a)	1.0651 (8)	0.6296 (9)	1.108 (1)	0.08 (1)
C(12a)	1.2638 (6)	0.8206 (9)	0.925 (1)	0.08 (1)	O(14a)	1.0088 (6)	0.6424 (7)	1.057 (1)	0.108 (8)
O(12a)	1.2608 (7)	0.8393 (8)	1.022 (1)	0.13 (1)	C(14b)	1.0867 (6)	0.639 (1)	1.234 (1)	0.13 (2)
C(12b)	1.3157 (6)	0.8503 (9)	0.8477 (9)	0.09 (1)	C(14c)	1.0239 (8)	0.651 (1)	1.309 (1)	0.141 (7)†
C(12c)	1.3762 (7)	0.884 (1)	0.918 (1)	0.153 (8)†	C(14d)	0.998 (1)	0.564 (1)	1.324 (2)	0.183 (9)†
C(12d)	1.4374 (9)	0.889 (2)	0.842 (2)	0.31 (2)†	C(15)	1.1345 (9)	0.4917 (8)	0.884 (2)	0.10 (1)
C(13)	1.1715 (6)	0.6423 (7)	0.871 (1)	0.056 (8)	O(15)	1.0786 (8)	0.4496 (7)	0.925 (1)	0.17 (1)
O(13)	1.1542 (4)	0.6408 (5)	0.7546 (7)	0.056 (5)	C(15a)	1.062 (1)	0.375 (1)	0.869 (2)	0.14 (2)
C(13a)	1.2054 (7)	0.6178 (9)	0.6808 (8)	0.066 (9)	O(15b)	1.0937 (9)	0.3397 (9)	0.790 (1)	0.15 (1)
O(13a)	1.2598 (6)	0.587 (1)	0.7089 (8)	0.13 (1)	C(15b)	0.998 (1)	0.335 (1)	0.901 (2)	0.20 (2)
C(13b)	1.1770 (5)	0.631 (1)	0.5609 (9)	0.09 (1)	C(15c)	0.979 (1)	0.365 (2)	1.023 (2)	0.22 (1)†
C(13c)	1.2358 (8)	0.6254 (9)	0.478 (1)	0.128 (6)†	C(15d)	1.039 (2)	0.340 (3)	1.105 (2)	0.32 (2)†

† Isotropic refinements.

perpendicular to the *a* axis. The alternating overlapping layers of molecules *A* and *B* are stacked in the **c** direction, and are infinitely linked parallel to the **b** direction with cyclic N(3)H···O(2) hydrogen-bond pairings between the adjacent molecules (Table 4), a very frequently observed hydrogen-bonding pattern in flavin (discussed later). On the other hand, two kinds of polar columns, which consist of adjacent ribityl groups of molecule *A* and molecule *B*, run along the **b** and **c** directions, respectively. The degree of packing the former column is more loose than that of the latter column, and this reflects the fact that (1) some acetyl esters in molecule *B* have large thermal motions and (2) the solvent acetone and water molecules are located only in the latter column, in order to strengthen the packing. Since all

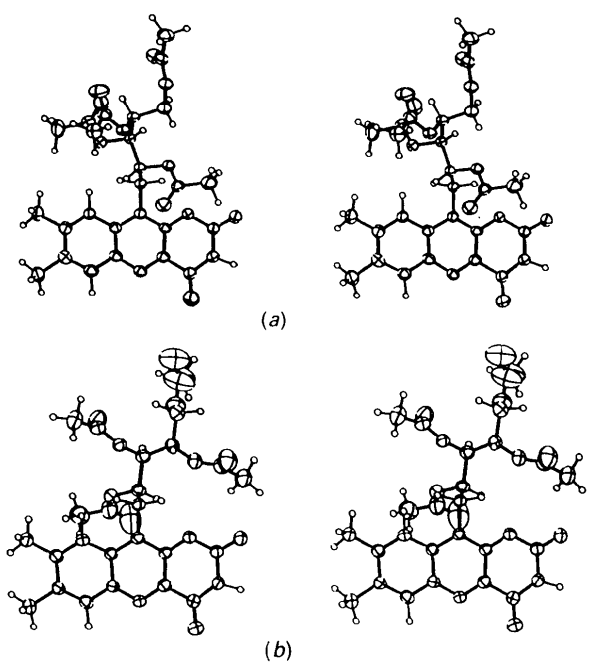

Fig. 2. Stereoscopic views of molecular conformations of RTAc molecule *A* (*a*) and molecule *B* (*b*).

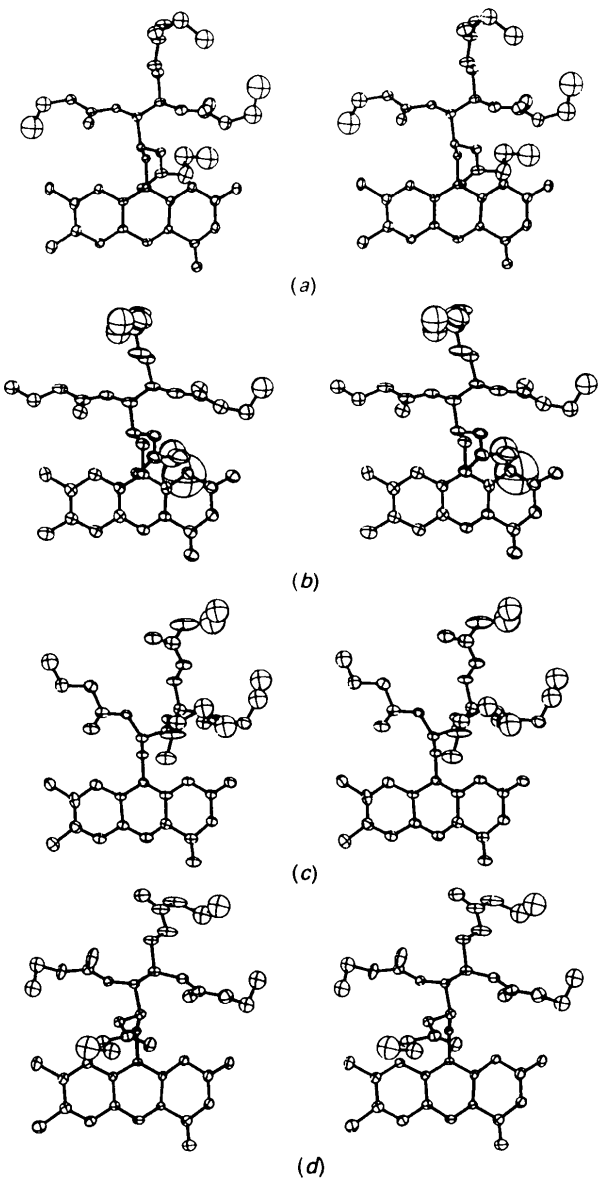

Fig. 3. Stereoscopic views of molecular conformations of RTB molecule *A* (*a*), molecule *B* (*b*), molecule *C* (*c*) and molecule *D* (*d*).

OH groups of the ribityl group are blocked as acetyl esters, there are no hydrogen bonds in the columns. The water molecules are located at the site at which the metal ion most frequently occurs in metal complexes of flavin derivatives (Langhoff & Fritchie, 1970) and are bound to the O(4) and N(5) atoms of the isoalloxazine ring of molecule *B* with a relatively weak interaction (Table 4). The water and acetone molecules are linked with an OH···O hydrogen bond; the acetone solvent stabilizes the molecular packing of molecule *B* by short contacts with the ribityl group.

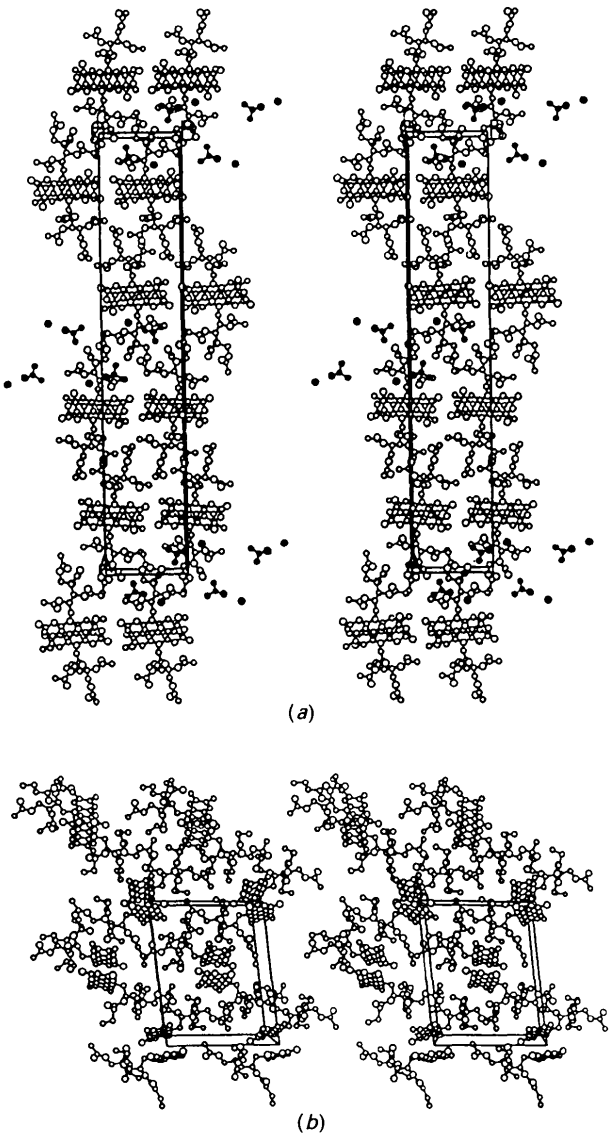

Fig. 4. Stereoscopic views of molecular packing of RTAc (*a*) and RTB (*b*) crystals. The water and acetone solvents in RTAc are shown with filled circles.

Conformational features and crystal packing of the RTB molecule

To the best of our knowledge, this is the first analysis of a crystal structure containing four crystallographically independent riboflavin conformers per asymmetric unit. Because of the relatively poor crystallinity of the RTB molecule (probably due to its

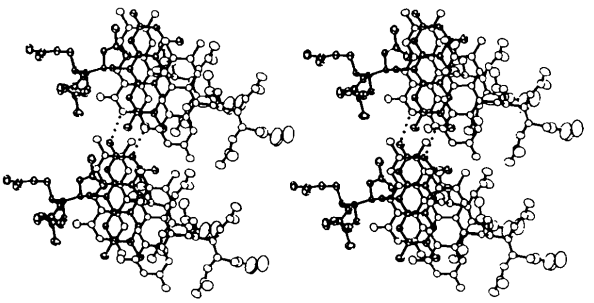

Fig. 5. Stereoscopic view of stacking and hydrogen-bonding interactions stabilizing the aggregation of RTAc isoalloxazine rings. The hydrogen bonds are shown by dotted lines. Molecule *A* is shown with ellipsoidal circles.

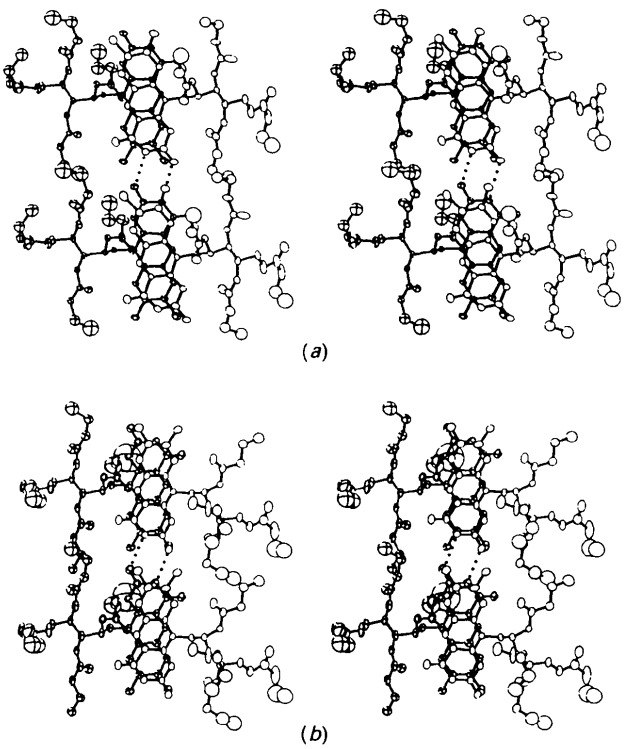

Fig. 6. Stereoscopic views of stacking and hydrogen-bonding interactions stabilizing the aggregation of RTB isoalloxazine rings of molecules *A* and *D* (*a*) and molecules *B* and *C* (*b*). The hydrogen bonds are shown by dotted lines. Molecules *A* and *B* are shown with ellipsoidal circles.

Table 3. *Selected torsion angles* (°) *around the ribityl conformation*

The e.s.d.'s for torsion angles are 0.3–0.4° for RTAc and 1° for RTB. The torsion angles χ_1 to χ_5 correspond to C(10a)—N(10)—C(11)—C(12), N(10)—C(11)—C(12)—C(13), C(11)—C(12)—C(13)—C(14), C(12)—C(13)—C(14)—C(15) and C(13)—C(14)—C(15)—O(15), respectively. Symbols *P* and *M* correspond to the torsion angles near to +90 and −90°, respectively. Symbols *t*, g^+ and g^- correspond to *trans*, *gauche*$^+$ and *gauche*$^-$ conformations, respectively.

	RTAc		RTB			
	Mol *A*	Mol. *B*	Mol. *A*	Mol. *B*	Mol. *C*	Mol. *D*
χ_1	−95.1(*M*)	88.9(*P*)	99(*P*)	107(*P*)	−92(*M*)	−87(*M*)
χ_2	−160.3(*t*)	−173.3(*t*)	174(*t*)	172(*t*)	92(g^+)	−171(*t*)
χ_3	−167.7(*t*)	62.3(g^+)	102(g^+)	101(g^+)	73(g^+)	−62(g^-)
χ_4	74.1(g^+)	175.8(*t*)	180(*t*)	178(*t*)	89(g^+)	−169(*t*)
χ_5	168.4(*t*)	−60.8(g^-)	63(g^+)	52(g^+)	−171(*t*)	−174(*t*)

Table 4. *Possible hydrogen-bond distances* (Å)

Donor at *x*, *y*, *z*	Acceptor at	Symmetry operation	Distance (Å)
RTAc			
N(3)*A*	O(2)*B*	*x*, *y* − 1, *z*	2.805 (5)
N(3)*B*	O(2)*A*	*x*, *y* + 1, *z*	2.864 (4)
O(1*W*)	O(4)*B*	*x*, *y* + 1, *z* + 1	3.191 (5)
O(1*W*)	N(5)*B*	*x*, *y* + 1, *z* + 1	3.259 (5)
O(1*W*)	O(1Ac)	*x*, *y*, *z*	2.994 (6)
RTB			
N(3)*A*	O(2)*D*	*x*, *y*, *z* − 1	3.04 (1)
N(3)*B*	O(2)*C*	*x*, *y*, *z* + 1	2.84 (2)
N(3)*C*	O(2)*B*	*x*, *y*, *z* − 1	2.96 (2)
N(3)*D*	O(2)*A*	*x*, *y*, *z* + 1	2.74 (2)

chemical structure), the present *R* value remains high and e.s.d.'s for the bonding parameters are somewhat large (0.02–0.04 Å for bond lengths and 0.6–2° for bond angles); although bond lengths and angles are almost in the usual region, C(15a)—O(15a) = 0.96 (5) Å is abnormally short. However, such uncertainty does not significantly affect the following discussion. The four independent isoalloxazine rings are planar to within −0.15 to 0.13 Å, and the atoms directly attached to the ring are almost in the plane.

The neighboring isoalloxazine rings consisting of molecules *A* and *D* and molecules *B* and *C* are extensively overlapped in an antiparallel mode and are linked head-to-tail *via* the usual N(3)H···O(2) hydrogen-bonded pairings to each other, thus forming two kinds of double-layered planar structures parallel to the **c** direction. In contrast to such tightly fixed isoalloxazine rings in the crystal, the ribityl side moieties occupy a large space for the crystal packing, and are located around the layers of isoalloxazine rings. These ribityl moieties are mainly held by van der Waals contacts. Since the ribityl OH's are all esterified with the butyryl groups, the possibilities for hydrogen-bond formation are very few in the present crystal without solvent molecules. This is the reason why the crystallinity of RTB was relatively poor and the ribityl side chain, especially the terminal butyryl groups, showed large thermal motions.

On the other hand, such a large space occupied by the ribityl moieties allows four different variations of the ribityl conformation. In order to avoid intramolecular short contacts among the butyryl groups, the ribityl backbone assumes a conformation suitable for each molecule, depending on the molecular packing environment. However, each conformation reflects the characteristics commonly observed in flavin derivatives (Table 3), as was stated above for the RTAc molecule. It is interesting to note that molecule *C* provides the first example of a ribityl moiety not showing a *trans* conformation (χ_2) about the C(11)—C(12) bond. Riboflavin and all its derivatives analyzed so far have exhibited the *trans* orientation for the χ_2 torsion angle, in spite of either the *M* or *P* conformation of χ_1, except for molecule *C*. Another common characteristic of flavin is also lacking in molecule *C*, *i.e.* the *trans* orientation intervenes between the *gauche*$^+$ and/or *gauche*$^-$ ones to allow the χ_2 to χ_5 torsion angles to avoid short contacts with the bulky side group. By taking a *gauche*$^+$ orientation of χ_2, molecule *C* adopts a conformation in which the extended butyryl ester connected to the ribityl C(12) atom is *trans* oriented to that connected to the C(15) atom, and locates nearly parallel to the isoalloxazine ring, while the rest of RTB adopts *trans* χ_2 torsion angles to form a *trans* zigzag butyl ester conformation at the ribityl C(13) atom with respect to that at C(14) atom, which runs nearly parallel to the isoalloxazine ring.

When the molecular conformations of the RTAc and RTB molecules are compared with each other, the conformational flexibility of the ribityl ester moiety appears to be limited, as the bulkiness of the ester group becomes large. The orientation of *P* or $M(\chi_1)\ -t(\chi_2)\ -g(\chi_3)\ -t(\chi_4)$ is thought to be preferable for RTB, while it would allow considerable variation in RTAc or similar flavin derivatives.

Stacking interactions and hydrogen-bonded dimer formation between isoalloxazine rings

A characteristic of the RTAc crystal structure is the extensive overlapping of isoalloxazine rings. This stacking mode is shown in Fig. 5, where the central molecule *A* is sandwiched between two neighboring *B* molecules related by translation of the *c* unit cell. The dihedral angle between molecules *A* and *B* is 1.03 (8)°, and the mean separation distance is 3.36 Å for the lower pair and 3.51 Å for the upper pair, where the interaction of the upper pair is less extensive. On the other hand, the stacking mode of the isoalloxazine rings of RTB is different from that in RTAc in such a way that two independent stacking pairs of molecules *A* and *D* and of molecules *B* and *C* are formed, as shown in Fig. 6. The dihedral angles and averaged interplanar spacings are 5.8 (3)°

and 3.379 Å for the former pair and 1.4 (3)° and 3.365 Å for the latter pair, respectively. Since such overlapping is most frequently observed in the crystal structures of riboflavin and its related compounds, it could be an energetically favorable packing mode for the isoalloxazine ring. Generally, the isoalloxazine rings are alternately stacked in such a way that the long axes of the respective rings are antiparallel; consequently, the dipole–dipole interaction becomes completely coupled. The antiparallel alignment of stacked isoalloxazine rings with an interplanar spacing less than the minimum van der Waals separation distance 3.4 Å indicates that partial π–π charge transfer between the rings has taken place even at the ground state, and could be thought of as being a major factor in stabilizing the molecular packing of RTAc and RTB crystals. It is conceivable that the orange color of the present *A*-type crystals is caused by such ring overlapping, and the polymorph of RTAc, characterized by its different crystal color, may result from a slight difference between the ring stacking modes. In addition to the stacking character, the isoalloxazine ring has a strong preference to form a cyclic dimer *via* N(3)H···O(2) hydrogen-bond pairing (Table 4 and Figs. 5 and 6). The combination of this hydrogen-bonding and stacking character leads to a large two-dimensional hydrophobic double layer.

This work was supported in part by the Office of Naval Research, Mechanics Division.

References

DEDAERDEMAEKER, T., GERMAIN, G., MAIN, P., TATE, C. & WOOLFSON, M. M. (1987). *MULTAN*87. *A System of Computer Programs for the Automatic Solution of Crystal Structures from X-ray Diffraction Data*. Univs. of York, England, and Louvain, Belgium.

EBITANI, M. (1987). *Yakugaku Zasshi*, **107**, 338–343.

EBITANI, M. (1988*a*). *Yakugaku Zasshi*, **108**, 39–43.

EBITANI, M. (1988*b*). *Yakugaku Zasshi*, **108**, 1141–1147.

EBITANI, M., KASHIWAGI, H., INOUE, M., ENOMOTO, S. & ISHIDA, T. (1989). *Chem. Pharm. Bull.* **37**, 2273–2275.

FUJII, S., KAWASAKI, K., SATO, A., FUJIWARA, T. & TOMITA, K. (1977). *Arch. Biochem. Biophys.* **181**, 363–370.

INOUE, M., SHIBATA, M., KONDO, Y. & ISHIDA, T. (1981). *Biochemistry*, **20**, 2936–2945.

ISHIDA, T. (1988). *Yakagaku Zasshi*, **108**, 506–527.

ISHIDATE, M. (1979). *Syokuhin Tenkabutsu Koteisyo Kaisetsusyo*, Vol. IV. Tokyo: Hirokawa.

KARPLUS, P. A. & SCHULZ, G. E. (1987). *J. Mol. Biol.* **195**, 701–729.

LANGHOFF, C. A. & FRITCHIE, C. J. JR (1970). *J. Chem. Soc. Chem. Commun.* pp. 20–21.

MCCORMICK, D. B. (1977). *Photochem. Photobiol.* **26**, 169–182.

MAYHEW, S. G. & LUDWIG, M. L. (1975). *The Enzymes*, Vol. 12, edited by P. D. BOYER, pp. 57–118. New York: Academic Press.

SCHRENDER, H. A., PRICK, P. A. J., WIERENGA, R. K., VRIEND, G., WILSON, K. S., HOL, W. G. J. & DRENTH, J. (1989). *J. Mol. Biol.* **208**, 679–696.

SCHULZ, G. E., SCHIRMER, R. H. & PAI, E. F. (1982). *J. Mol. Biol.* **160**, 287–308.

SHELDRICK, G. M. (1980). *SHELXTL*80. *An Integrated System for Solving, Refining and Displaying Crystal Structures from Diffraction Data*. Univ. of Göttingen, Germany.

The Universal Crystallographic Computing System – Osaka (1979). The Computation Center, Osaka Univ., Japan.

VRIELINK, A., LLOYD, L. F. & BLOW, D. M. (1991). *J. Mol. Biol.* **219**, 533–554.